

**Simulation studies of the HADES first level
trigger.
PART I: Performance in heavy-ion induced
reactions**

R. Schicker¹ and H. Tsertos

University of Cyprus, Nicosia, Cyprus

Abstract

The first level trigger of the HADES spectrometer is studied for the heavy-ion collision systems Au+Au and Ne+Ne. The trigger efficiency for central events is given in dependence of the imposed charged particle multiplicity condition. The timing properties of the trigger signal are described. The losses due to deadtime are specified. Finally, the first level trigger rate is reported.

¹ Corresponding author, e-mail "schicker@alpha2.ns.ucy.ac.cy"
Dept. Nat. Science, Univ. Cyprus, PO 537, 1678 Nicosia, Cyprus

1 Introduction

The dilepton spectrometer HADES is currently being built at the heavy-ion synchrotron SIS at GSI Darmstadt[1]. HADES will measure dielectron pairs emitted in relativistic heavy-ion collisions in the beam energy range of 1-2 AGeV. Additionally, a secondary pion beam facility of momenta between 0.5 GeV/c and 2.5 GeV/c will allow the measurements of dilepton observables in pion induced reactions[2]. Measurements of in-medium dielectron decays of the vector mesons ρ , ω and ϕ allow to reconstruct in-medium masses of these vector mesons. Hence, experiments with HADES will test a series of conjectures about in-medium behavior of vector mesons in hot and dense matter produced in relativistic heavy-ion collisions[3].

The HADES spectrometer consists of a superconducting toroidal magnet with six sectors of 60° azimuthal angle each. The acceptance in polar angle extends from 18° to 85° in the forward hemisphere. Multiwire Drift Chambers (MDCs) placed forward of and behind the magnetic field are used for trajectory reconstruction of the individual particles. Between the target and magnetic field region, a Ring Imaging Cherenkov detector (RICH) identifies electron trajectories with a threshold $\gamma_{thr} \sim 20$. In the region behind the magnetic field, a second, independent electron identification is achieved by a Multiplicity/Electron Trigger Array (META). The META system consists of time of flight (TOF) paddles and shower detectors[1].

HADES is designed to operate at heavy-ion beam intensities of 10^8 particles per second. A 1% interaction target results in 10^6 minimum bias events per second. The multi-level trigger system of HADES has to reduce this primary rate to a few hundred events per second which will be written onto tape. The first level trigger is designed to select central collisions by recognizing events with a large charged particle multiplicity. The expected rate of the first level trigger is 10^5 events per second. The second level trigger searches for lepton candidates by matching the identified RICH rings with the measured META showers. This matching procedure is based on the angular correlations of physical tracks in the RICH and META detectors. The third level trigger combines the output of the matching unit with the tracking information from the MDCs. This trigger stage rejects mainly combinations of low energy electrons producing a RICH ring with hadrons misidentified as leptons in the META system.

The purpose of this paper is to present simulation studies of the HADES first level trigger in heavy-ion induced reactions. Simulation results are shown for the systems Au+Au at 1 AGeV and Ne+Ne at 2 AGeV, in order to illustrate the trigger performance in a heavy and a light collision system, respectively.

This paper is organized as follows: Section 2 gives a summary on the HADES first level trigger requirements. In Section 3, the simulation of the first level trigger data is described. Section 4 introduces the analysis of the simulation data. In Section 5, the performance characteristics of the first level trigger in the heavy system Au+Au is presented. Section 6 gives details of the first level trigger performance in the light system Ne+Ne.

2 First level trigger requirements

The HADES first level trigger will tag central heavy-ion reactions by recognizing events with a large charged particle multiplicity. This multiplicity can be derived from the highly segmented TOF array. A lower limit on the number of TOF paddles carrying a signal will select central events. An optimal first level trigger accepts all central events while suppressing non-central events as much as possible.

Comprehensive dilepton spectroscopy of heavy-ion reactions, however, necessitates additionally the measurement of the dielectron signal in non-central events. With the same first level trigger approach as described below, data of non-central events can be taken by redefining the multiplicity conditions and by appropriately downscaling the resulting trigger rate. Thus, non-central events can either be downscaled and be registered simultaneously with central events or can be recorded in dedicated data taking periods.

The trigger signal derived from the multiplicity conditions of the TOF paddles is used as gate for the ADCs of the RICH detector and as common STOP for the TDCs. Hence the delay of this signal with respect to the time of reaction as well as the time jitter are of particular interest. The time jitter of the first level trigger signal arises from different sources. First, trajectory length variations over the polar angular range of the spectrometer induce particle time of flight variations. Second, velocity variations of the particles defining the trigger transition add to the time of flight variations. Third, the different signal propagations in the TOF paddles depending on location of the hit point add varying delays to the TOF signals.

Each signal of the first level trigger has an associated deadtime due to frontend readout of detectors. This deadtime is about 10 μ sec. If the multiplicity condition is set low, then the trigger rate will be increased with a corresponding increase in probability that central events fall into the deadtime window. If, on the other hand, the multiplicity condition is set high, then central events start to get rejected due to insufficient multiplicity. For a given deadtime, there exists therefore a multiplicity condition which optimizes the number of central events which are passed onto the next trigger stage.

Due to the statistical occurrence of heavy-ion reactions, there is a finite probability that two or more events occur very close in time. Hence, TOF paddles can carry simultaneously signals of different events. The combined signals of the different events may satisfy the trigger condition whereas none of the individual events would be able to do so. This overlap probability depends strongly on the reaction rate and, thus, on beam intensity. For all of the results shown, a beam rate of 10^8 per second and a minimum bias event rate of 10^6 per second is assumed.

The performance of the first level trigger in heavy-ion collisions depends weakly on the duration of the TOF paddle signals[4,5]. If the TOF signal length is short, the signals from the fastest particles will have disappeared, while the signals from the slower particles of the event have not started yet. The trigger system will therefore see an apparently reduced event multiplicity. TOF signals which are long, on the other hand, result in an increased number of triggers from events overlapping in time. In this report, all the results shown have been derived with a TOF signal duration of 15 nsec.

3 First level trigger data simulation

For studying the behavior of the first level trigger, the full HADES geometry was implemented into the GEANT package[6]. A realistic field map of the toroidal magnetic field is used for tracking of the charged particles.

The collisions of the two systems studied Au+Au and Ne+Ne are modeled by a transport equation of the Boltzmann-Uehling-Uhlenbeck (BUU) type. The dynamical evolution of the collisions is determined by calculating the phase space evolution for nucleons, Delta and N^* resonances. With this code, good agreement is found between data and model predictions for nucleon, pion, kaon and dilepton distributions in heavy-ion collisions in the energy range 1-2 AGeV[7]. Since the charged particle multiplicity in central collisions is mainly due to protons and pions, only these two particle species are tracked for the first level trigger simulations.

For the simulations of the first level trigger in the systems Au+Au and Ne+Ne, BUU events of different impact parameters are used. In these systems, the upper limit of the impact parameter range is defined by the geometrical cross section. In each of the two systems studied, six to eight discrete equidistant impact parameters represent the full range from zero to maximum value. Each tracked particle of an event is followed through the complete HADES geometry. A trajectory entering a TOF paddle volume defines a TOF hit. The information of this hit contains the TOF paddle number and a time value. This time value represents the sum of the particles time of flight from tar-

get to the paddle hit point plus the shorter of the two propagation delays of the signal to either end of the paddle. Here, no finite resolution or signal time jitter is assumed. This exact time value is then converted into an integer format with a discretization accuracy of 10 psec and subsequently written into a CERN CWN-tupel. At this stage, each discrete impact parameter is simulated separately. Hence, separate tuple files exist for each of the discrete impact parameters simulated.

4 First level trigger data analysis

In the analysis of the first level trigger, a stream of events is generated by assigning a random time interval t_{Δ} and a random impact parameter b to each event.

The time interval t_{Δ} is chosen according to the probability $p(t_{\Delta}) = \lambda \cdot e^{-\lambda \cdot t_{\Delta}}$. This probability distribution represents the distribution of time intervals between two consecutive events, with λ being equal to the inverse of the average time between two consecutive events. The absolute time of an event is determined by adding t_{Δ} to the absolute time of the previous event.

The impact parameter b of an event is taken from a distribution which is zero at $b = 0$ fm and linearly increasing up to $b = b_{max}$. Here, b_{max} is defined by the geometrical cross section as explained above. An event is subsequently read from the tuple file with the closest nearby simulated impact parameter.

The analysis of the first level trigger loops over all TOF paddles in time steps of 1 nsec. In each loop, the sum of the TOF paddles carrying a signal at that particular moment is calculated. If the given trigger multiplicity requirement is met in a step, but not in the previous one, then a trigger transition is induced. In the prompt trigger described below, a trigger transition generates a trigger. In the delayed trigger described below, a trigger transition initiates a time window of 20 nsec during which the event has to satisfy an additional multiplicity requirement. If this additional condition is met, then a trigger is generated. Here, prompt and delayed trigger refer to the one and two step trigger approach as described in Section 5.7. Each trigger starts a deadtime window during which no other triggers are accepted.

5 First level trigger in Au+Au collisions

5.1 Sector multiplicity condition

In the high multiplicity heavy-ion system Au+Au, a multiplicity condition in each azimuthal sector will tag central events. Fig. 1 shows the tagging efficiency for this system as a function of the imposed sector multiplicity condition M_S . This condition implies that the charged particle multiplicity is greater or equal to M_S in each of the six azimuthal sectors. Shown are the data points for events with impact parameters of 1,3 and 5 fm, respectively. For all the impact parameters shown in Fig. 1, the efficiency exhibits a plateau of nearly 100% at low sector multiplicity values but drops steeply at large multiplicity values. The optimal choice for the sector multiplicity condition is a value as large as possible but still within the plateau of the impact parameter $b = 1$ fm. Hence, the sector multiplicity condition is set to $M_S \geq 8$ for the calculations shown below.

5.2 Trigger timing

Events satisfying the sector multiplicity condition M_S generate a trigger transition. The delay of this signal relative to the time of reaction and the signal jitter are of interest. Fig. 2 shows the timing of the trigger transition for events with different impact parameters. Central events are represented by the solid line. The FWHM of their time distribution amounts to about 2 nsec. The FWHM value for events with impact parameters of 3 and 5 fm are about 4 and 6 nsec, respectively. Semi-central events meet the trigger condition only with the help of slower moving particles. Hence, for increasing impact parameters, a shift of the centroid to larger time values as well as a broadening of the distribution is seen. The time zero in Fig. 2 is the time of reaction.

5.3 Total multiplicity

The sector multiplicity requirement defines a condition on minimum particle multiplicity in each of the six azimuthal sectors. A condition on minimum total multiplicity might further reduce non-central events while at the same time accepting all central events. At the moment of the trigger transition, the total multiplicity for central events is still building up, whereas it is almost exhausted for non-central events. Fig. 3 displays the maximum total multiplicity reached during a time window of 20 nsec following the trigger transition. Central and non-central events which satisfy the sector multiplicity condition M_S behave quite differently in Fig. 3. A condition on minimum total multiplicity will therefore further reduce non-central events.

5.4 Timing total multiplicity

Fig. 4 shows the time at which the maximum event multiplicity is reached for events with impact parameters $b=1,3$ and 5 fm. Here, the time zero is the time of the trigger transition defined by the sector multiplicity condition M_S . For central events, the maximum total multiplicity develops between 5 and 15 nsec following the trigger transition. Non-central events with impact parameters $b=5$ fm develop their maximum total multiplicity during a time span of about 10 nsec following the trigger transition. Hence a time window of 15-20 nsec duration following the trigger transition seems adequate to test for the maximum total event multiplicity.

5.5 Trigger efficiency

Each trigger transition followed by a total multiplicity larger than a required minimum value M_T generates a trigger. Each trigger has an associated deadtime due to frontend readout of electronic channels. An event trigger occurring during the deadtime window of the previous trigger will not initiate readout and the information of the event is lost. Fig. 5 shows the values of $\text{Eff}_{LV1} \times R_{DT}$ for central events for $M_S \geq 8$ as a function of the required total multiplicity M_T . Here, Eff_{LV1} denotes the first level trigger efficiency, i.e., the efficiency for zero deadtime. R_{DT} is a reduction factor which contains the effects of the trigger deadtime. For the deadtime of 10 μsec , the $\text{Eff}_{LV1} \times R_{DT}$ value has a maximum at an M_T value of about 110. At lower M_T values, semi-central events do not get suppressed efficiently. Thus, the increased rate of semi-central events leads to a decrease of the $\text{Eff}_{LV1} \times R_{DT}$ values of central events. For high M_T values, $\text{Eff}_{LV1} \times R_{DT}$ decreases since central events start to get rejected due to insufficient multiplicity. The data for the deadtime of 6 μsec are shown for comparison.

5.6 Trigger rate

Table 1 lists the trigger rates in units of 10^5 per second for the different total multiplicity thresholds M_T and for deadtimes of $T_0 = 0,6$ and 10 μsec , respectively. A first level trigger rate of 1×10^5 per second is the input design value for the next trigger stage. Each T_0 value in Table 1 corresponds to two columns. The left column shows the rate of trigger transitions resulting from the sector multiplicity condition $M_S \geq 8$. The right column displays the rate if additionally the total multiplicity condition M_T is required.

Table 2 lists the partial trigger rates from events of different impact parame-

ters. For the chosen multiplicity requirements, triggers from events with impact parameters $b \geq 5$ fm are negligible and therefore not listed in Table 2. Both impact parameters $b = 1$ and 3 fm correspond to two columns. On the left, the partial trigger rate is shown in units of 10^5 per second. On the right, the partial rates are normalized to the total trigger rate and shown in units of percent.

5.7 First level trigger based on M_T

The trigger scheme studied so far divides the first level trigger into two consecutive steps: In a first step, the M_S fastest particles in each sector define the trigger timing by establishing a trigger transition. In a second step, the trigger transition is asserted or rejected within a subsequent time window depending on whether the total multiplicity condition M_T is satisfied. However, a one step trigger scheme, based exclusively on the total multiplicity M_T , seems also feasible since the total multiplicity condition M_T is more restrictive than the sector multiplicity condition M_S .

Fig. 6 displays the trigger timing achieved by the one and two step trigger. The solid line shows the timing in the two step scheme with conditions $M_S \geq 8$ and $M_T \geq 110$ as explained above. These data points correspond to Fig. 2 with the additional condition of total multiplicity M_T . The FWHM of this distribution is about 2 nsec. The dashed line in Fig. 6 represents the timing in the one step trigger. Here, the total multiplicity condition $M_T \geq 110$ defines the trigger. As expected, the timing is delayed compared to the two step trigger and considerably broadened. The FWHM of this distribution is about 6 nsec. The data shown in Fig. 6 represent the timing of all events which generate a trigger, irrespective of impact parameter.

6 First level trigger in Ne+Ne collisions

6.1 Minimum total multiplicity

Due to the low multiplicity of the Ne+Ne system, a substantial fraction of central events has no charged tracks in one or more of the azimuthal sectors. Hence even the lowest sector multiplicity condition of one particle per sector results in a low efficiency for Ne+Ne events. In order to define the trigger transition, the sector multiplicity condition used in the Au+Au system is therefore replaced by a minimal total multiplicity condition M_L . Fig. 7 shows the trigger efficiency for Ne+Ne events as a function of the total multiplicity

condition M_L . Shown are the data points for events with impact parameters of 1,2 and 3 fm, respectively. For all the impact parameters shown in Fig. 7, the efficiency exhibits a plateau of nearly 100% at low total multiplicity values but drops steeply at large values. The optimal choice for the low total multiplicity condition is a value as large as possible but still within the plateau of the impact parameter $b = 1$ fm. Hence, the low multiplicity condition is set to $M_L \geq 6$ for the calculations shown below.

6.2 Trigger timing

Fig. 8 shows the timing of the trigger transition for events with different impact parameters. Here, the trigger transition is defined by the condition of minimum total multiplicity $M_L \geq 6$. Events with impact parameter $b = 1$ fm are represented by the solid line. The FWHM of their time distribution amounts to about 2 nsec. The FWHM value for events with impact parameters of 2 and 3 fm are about 3 and 4 nsec, respectively. Semi-central events meet the trigger condition only with the help of slower moving particles. These slow particles result in the asymmetric tail of the time distribution seen in Fig. 8.

6.3 Total multiplicity

The low total multiplicity requirement M_L defines a condition on minimum total particle multiplicity. As in the Au+Au system, an additional condition on maximum event multiplicity developing within a time window following the trigger transition might further reduce non-central events. Fig. 9 displays the maximum total multiplicity M_H reached during a time window of 20 nsec following the trigger transition. Here, events with impact parameters $b=1,2$ and 3 fm develop different total event multiplicities. An additional condition on maximum event multiplicity reduces semi-central events considerably while affecting central events only little.

6.4 Timing total multiplicity

The time at which the maximum event multiplicity M_H is reached needs to be known if an additional condition on total multiplicity M_H is to be applied. Here, the time zero is the time of the trigger transition defined by the low total multiplicity condition M_L . Central and non-central events develop their maximum total multiplicity within a time span of 15 nsec following the trigger transition. Hence, similarly to the Au+Au system, a time window of 15-20 nsec

after the trigger transition seems adequate to test for the maximum total event multiplicity.

6.5 Trigger efficiency

In the Ne+Ne system, deadtime losses are treated in the same way as in the system Au+Au. Fig. 10 shows the values $\text{Eff}_{LV1} \times R_{DT}$ for central events as a function of the required total multiplicity M_H . The data points for zero deadtime represent the first level trigger efficiency. For the deadtime of 10 μsec , the $\text{Eff}_{LV1} \times R_{DT}$ value has a maximum at an M_H value of about 11. For the calculations shown below, the total multiplicity condition is therefore set to $M_H \geq 11$. At lower M_H values, semi-central events do not get suppressed efficiently. Hence the increased rate of semi-central events leads to a decrease of the $\text{Eff}_{LV1} \times R_{DT}$ values of central events. At high M_H values, $\text{Eff}_{LV1} \times R_{DT}$ decreases since central events are rejected due to insufficient multiplicity. The data for the deadtime of 6 μsec are shown for comparison.

6.6 Trigger rate

Table 3 lists the trigger rates for the Ne+Ne system. These rates are shown in units of 10^5 per second for the different total multiplicity thresholds M_H and for deadtimes of $T_0 = 0,6$ and 10 μsec , respectively. A first level trigger rate of 1×10^5 per second is the input design value for the next trigger stage. Each T_0 value in Table 3 corresponds to two columns. The left column shows the rate of trigger transitions resulting from the low total multiplicity condition $M_L \geq 6$. The right column displays the rate if additionally the total multiplicity condition M_H is required.

Table 4 lists the partial trigger rates from events of impact parameters $b = 1,2$ and 3 fm. Every impact parameter corresponds to two columns. On the left, the partial trigger rate is shown in units of 10^5 per second. On the right, the partial rates are normalized to the total trigger rate and shown in units of percent.

6.7 First level trigger based on M_H

As in the Au+Au system, a direct one step trigger scheme is also feasible in the Ne+Ne system. Fig. 11 shows the trigger timing achieved by the one and two step trigger based on multiplicity conditions of $M_L \geq 11$ and $M_L \geq 6$, $M_H \geq 11$, respectively. The solid line shows the timing in the two step scheme

as explained above. These data points correspond to Fig. 8 with the additional condition of total multiplicity $M_H \geq 11$. The FWHM of this distribution is about 2 nsec. The dashed line in Fig. 11 represents the timing in the one step trigger. Here, the total multiplicity condition $M_L \geq 11$ defines the trigger. As expected, the timing is delayed compared to the two step trigger and considerably broadened. This distribution has a FWHM of about 6 nsec and an asymmetric tail at the high value side. The data shown in Fig. 11 represent the timing of all events which generate a trigger, irrespective of impact parameter.

7 Conclusions

Simulations of the HADES first level trigger in both heavy-ion systems Au+Au and Ne+Ne indicate that the first level trigger can be implemented in both a one or two step trigger architecture. While both approaches yield the same trigger rate, the two step scheme results in a considerably improved timing of the trigger signal derived from the multiplicity conditions imposed on the TOF paddles. The two step scheme requires different multiplicity definitions for establishing the trigger transition in the two systems studied. A sector multiplicity condition is applied in the high multiplicity system Au+Au, but a requirement on total multiplicity is needed in the low multiplicity system Ne+Ne. By judicious choice of multiplicity specification for asserting the trigger transition, the number of central collisions passed onto the next trigger stage can be maximized. The trigger rate resulting from such multiplicity provisions satisfies the second level trigger requirement of 10^5 events per second in both the Au+Au and Ne+Ne systems.

Acknowledgements

The support of the lepton group at GSI and, in particular, fruitful discussions with W.Koenig are gratefully acknowledged. The authors thank Gy.Wolf for providing the BUU data files used in the simulations.

References

- [1] The HADES collaboration, Proposal for a High Acceptance Di-Electron Spectrometer, GSI 1994;
R.Schicker et al., Nucl. Instr. and Meth. A 380 (1996) 586
- [2] V.Metag, π N Newsletter 11, Vol.2 (1995), 159
- [3] G.E.Brown and M.Rho, Phys.Rev.Lett. 66 (1991) 2720;
G.E.Brown and M.Rho, Phys.Rep. 269 (1996) 333
- [4] R.Schicker and H.Tsertos, University of Cyprus preprint UCY-96/04
- [5] R.Schicker and H.Tsertos, University of Cyprus preprint UCY-96/08
- [6] H.Schön, PhD thesis, University of Frankfurt, 1996
- [7] G.Wolf, W.Cassing and U.Mosel, Nucl.Phys. A552 (1993) 549

Figure Captions

Fig. 1. First level trigger efficiency for the system Au+Au at 1 AGeV as a function of the sector multiplicity condition M_S . Shown are data points for events with impact parameters of $b=1,3$ and 5 fm.

Fig. 2. Trigger timing of first level trigger signal for impact parameters $b=1,3$ and 5 fm. The time zero is the time of reaction.

Fig. 3. The maximum total event multiplicity for impact parameters $b=1,3$ and 5 fm reached during a time window of 20 nsec following the trigger transition.

Fig. 4. Time at which the maximum total event multiplicity is reached for impact parameters $b=1,3$ and 5 fm. The time zero is the time of trigger transition.

Fig. 5. Efficiency of first level trigger (deadtime losses included) for central events. Shown are the data points as a function of the total multiplicity condition M_T for deadtimes of 0,6 and 10 μ sec.

Fig. 6. Trigger timing in the one (dashed line) and two step (solid line) trigger scheme (see text). The time zero is the time of reaction.

Fig. 7. First level trigger efficiency for the system Ne+Ne at 2 AGeV as a function of the minimum total multiplicity M_L . Shown are data points for events with impact parameters of $b=1,2$ and 3 fm.

Fig. 8. Trigger timing of first level trigger signal for impact parameters $b=1,2$ and 3 fm. The time zero is the time of reaction.

Fig. 9. The maximum total event multiplicity for impact parameters $b=1,2$ and 3 fm reached during a time window of 20 nsec following the trigger transition.

Fig. 10. Efficiency of first level trigger (deadtime losses included) for central events. Shown are the data points as a function of the total multiplicity condition M_H for deadtimes of 0,6 and 10 μ sec.

Fig. 11. Trigger timing in the one (dashed line) and two step (solid line) trigger scheme (see text). The time zero is the time of reaction.

Tables

Au + Au	$T_0 = 0 \mu\text{sec}$		$T_0 = 6 \mu\text{sec}$		$T_0 = 10 \mu\text{sec}$	
	rate [10^5]		rate [10^5]		rate [10^5]	
$M_T \geq 100$	1.08	.371	.896	.308	.794	.276
$M_T \geq 105$	1.08	.277	.939	.242	.853	.222
$M_T \geq 110$	1.08	.189	.980	.172	.914	.162
$M_T \geq 115$	1.08	.133	1.01	.124	.965	.118
$M_T \geq 120$	1.09	.081	1.04	.077	1.01	.075

Table 1

Rates of first level trigger transitions (left column) and of triggers (right column) in the system Au+Au (see text). The rates are shown in units of 10^5 per second for deadtimes $T_0 = 0, 6$ and $10 \mu\text{sec}$ and for different total multiplicity conditions M_T .

Au + Au	rate b=1fm		rate b = 3 fm	
	[10^5]	[%]	[10^5]	[%]
$M_T \geq 100$.110	39.7	.165	59.8
$M_T \geq 105$.113	51.0	.108	48.6
$M_T \geq 110$.113	69.5	.048	29.9
$M_T \geq 115$.095	80.3	.023	19.0
$M_T \geq 120$.068	90.3	.006	8.7

Table 2

First level partial trigger rates of events with impact parameters $b = 1$ and 3 fm in the system Au+Au for different total multiplicity conditions M_T . The left column displays the partial rate in units of 10^5 per second. In the right column, the partial rates are normalized to the total trigger rate and shown in units of percent.

Ne + Ne	$T_0 = 0 \mu\text{sec}$		$T_0 = 6 \mu\text{sec}$		$T_0 = 10 \mu\text{sec}$	
	rate [10^5]		rate [10^5]		rate [10^5]	
$M_H \geq 7$	2.20	1.85	1.05	.884	.774	.651
$M_H \geq 9$	2.21	1.30	1.26	.735	.966	.567
$M_H \geq 11$	2.22	.865	1.47	.574	1.19	.464
$M_H \geq 13$	2.22	.532	1.69	.408	1.45	.350
$M_H \geq 15$	2.22	.290	1.90	.248	1.73	.226

Table 3

Rates of first level trigger transitions (left column) and of triggers (right column) in the system Ne+Ne (see text). The rates are shown in units of 10^5 per second for deadtimes $T_0 = 0, 6$ and $10 \mu\text{sec}$ and for different total multiplicity conditions M_H .

Ne + Ne	rate b=1fm		rate b = 2 fm		rate b = 3 fm	
	[10^5]	[%]	[10^5]	[%]	[10^5]	[%]
$M_H \geq 7$.135	20.7	.215	33.0	.209	32.0
$M_H \geq 9$.155	27.3	.225	39.6	.149	26.3
$M_H \geq 11$.164	35.4	.197	42.5	.089	19.2
$M_H \geq 13$.159	45.4	.141	40.2	.046	13.0
$M_H \geq 15$.122	54.2	.082	36.4	.019	8.3

Table 4

First level partial trigger rates of events with impact parameters $b = 1, 2$ and 3 fm in the system Ne+Ne for different total multiplicity conditions M_H . The left column displays the partial rate in units of 10^5 per second. In the right column, the partial rates are normalized to the total trigger rate and shown in units of percent.

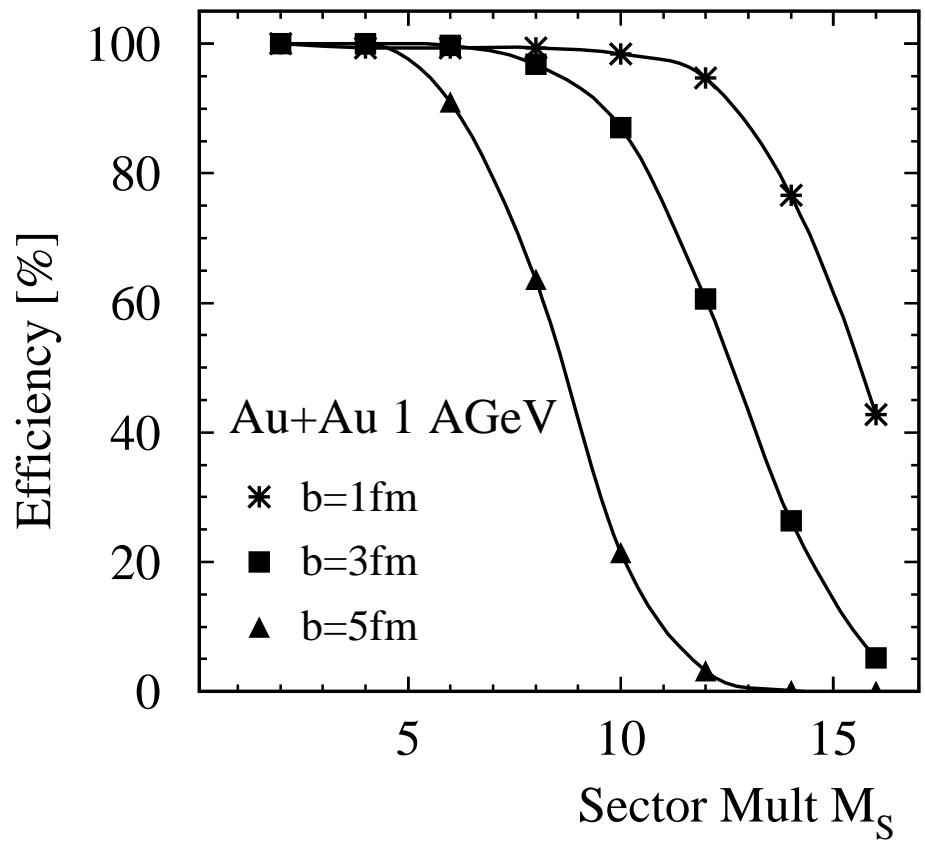


FIG.1

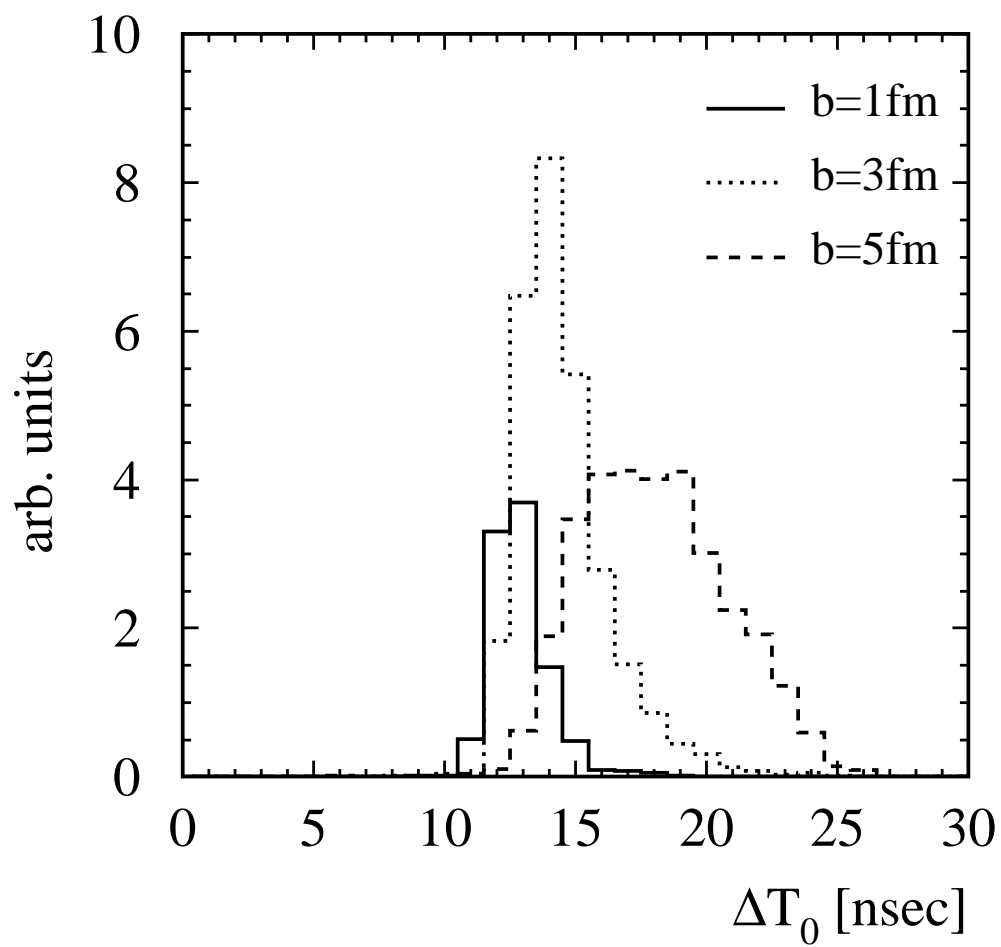


FIG.2

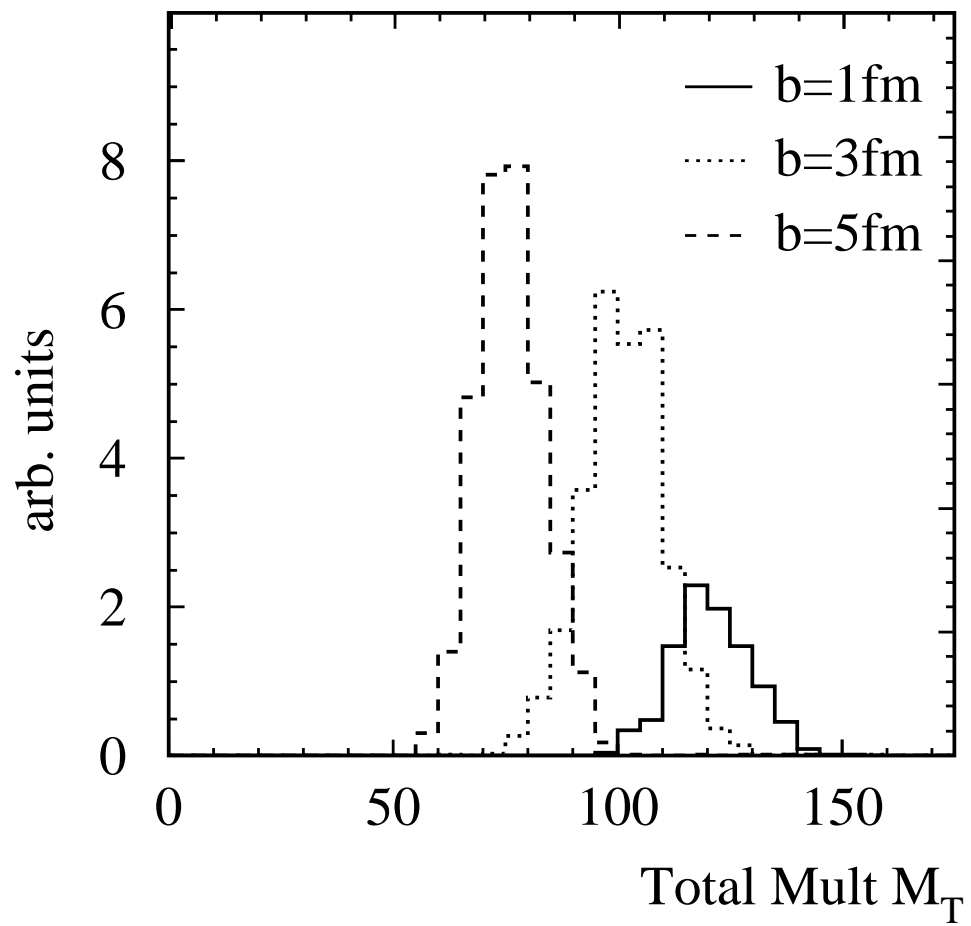


FIG.3

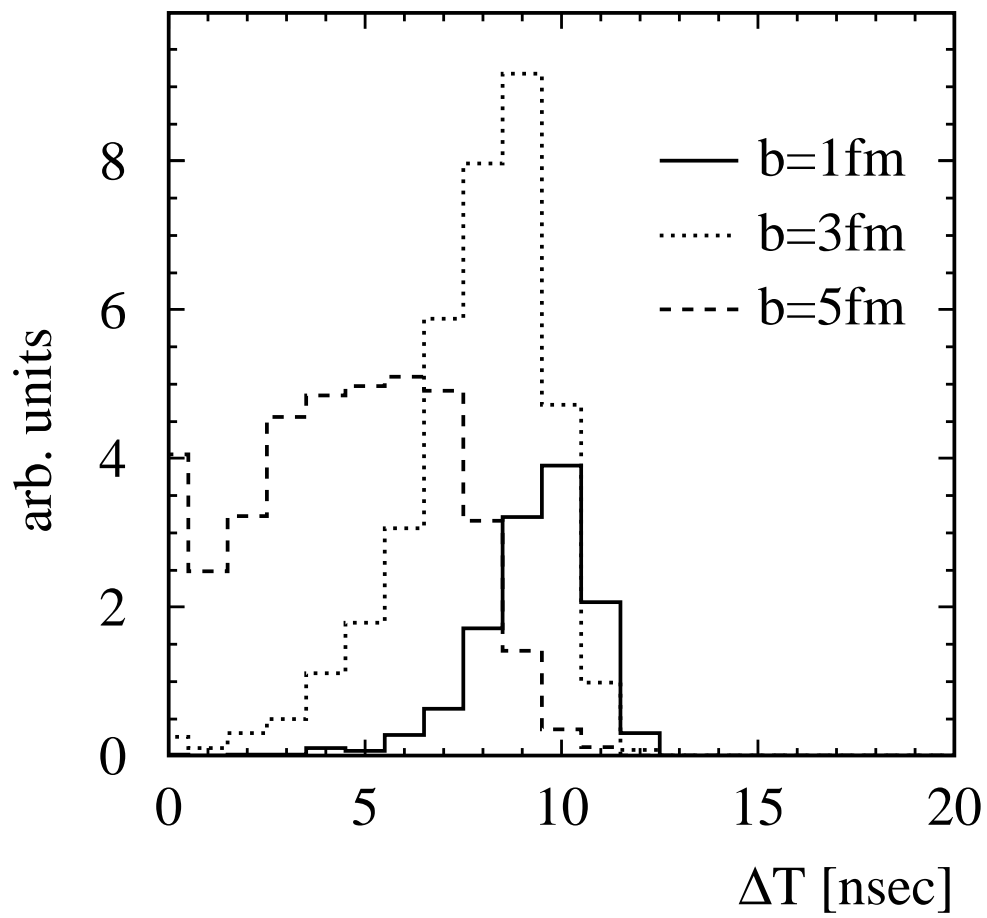


FIG.4

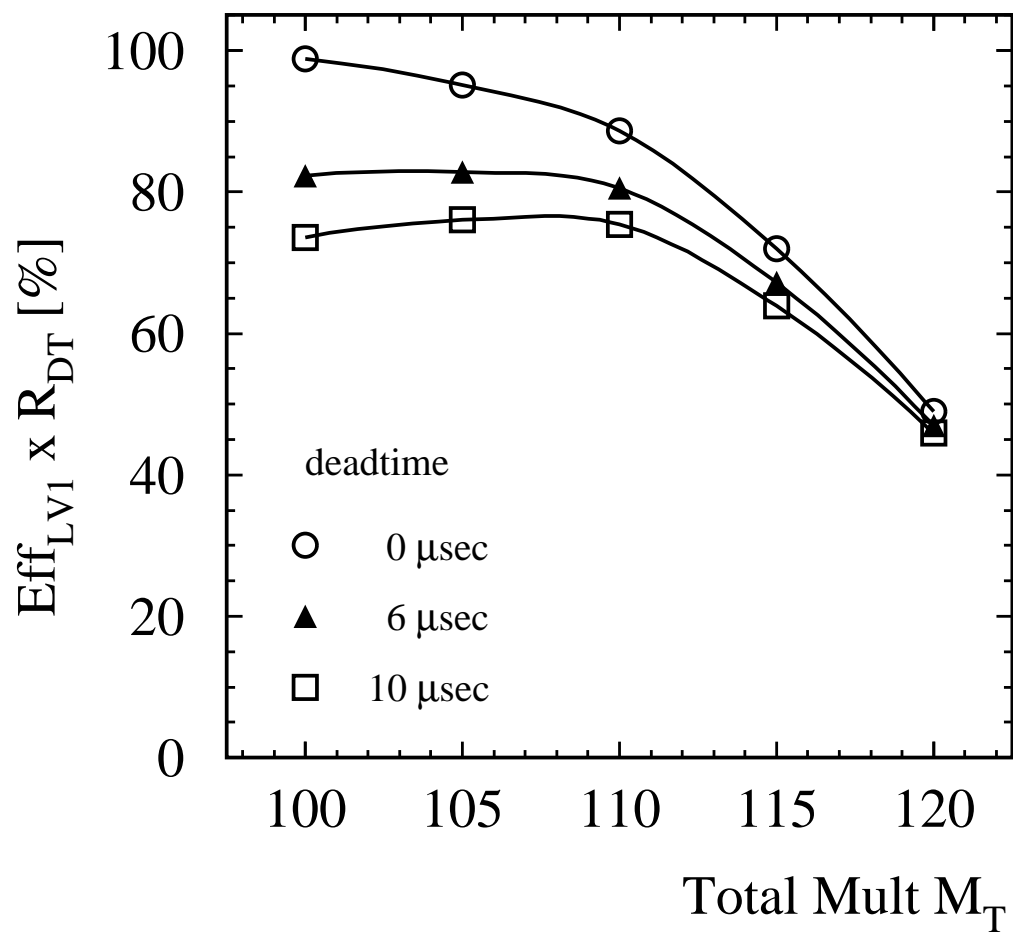


FIG.5

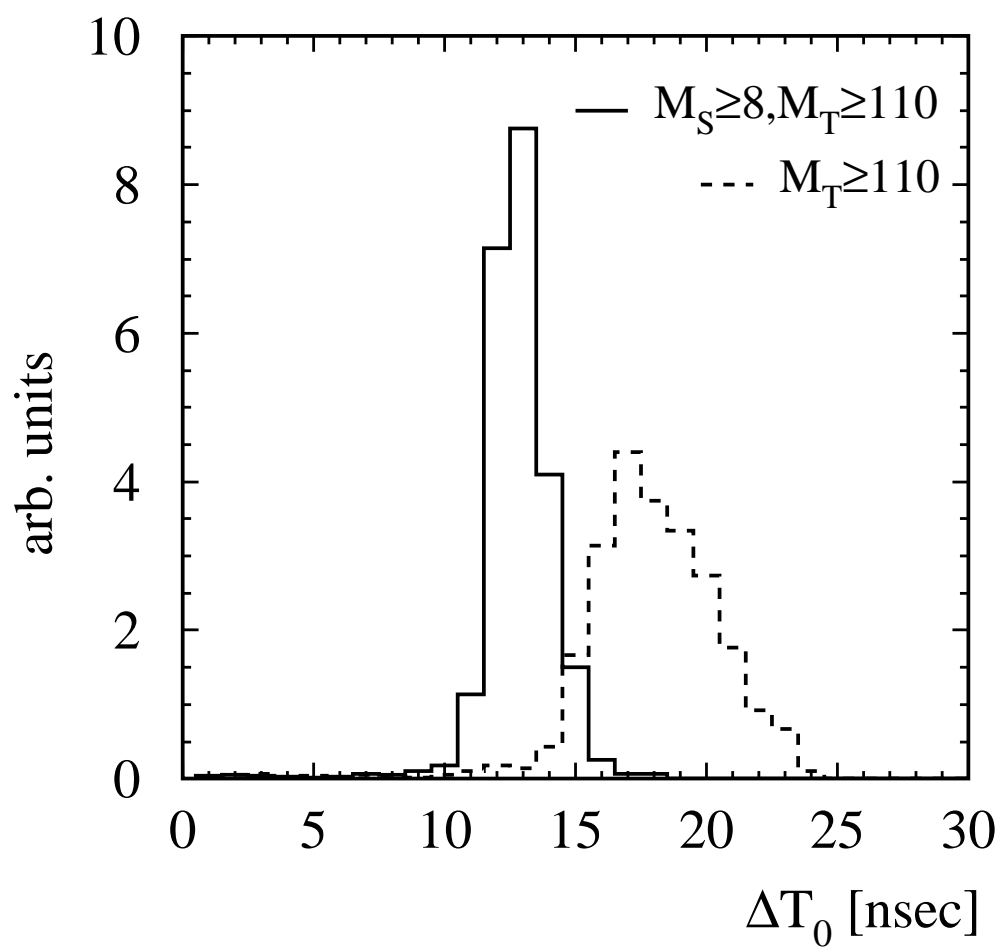


FIG.6

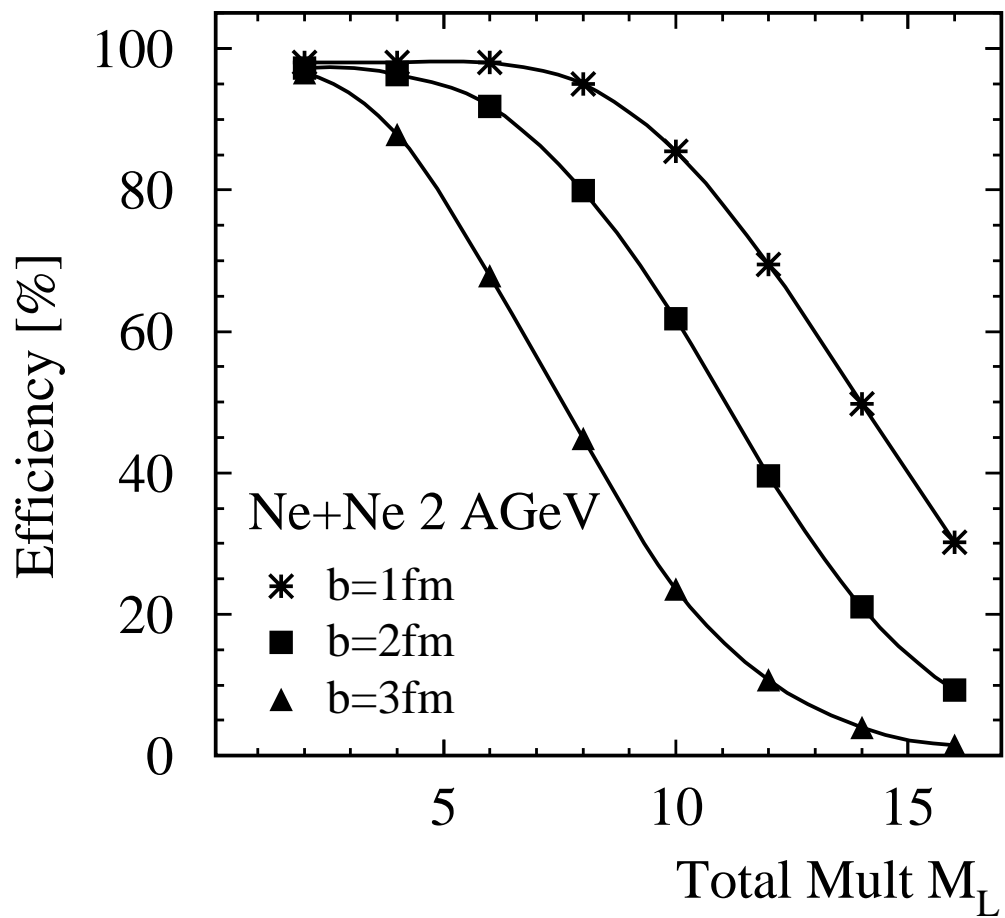


FIG.7

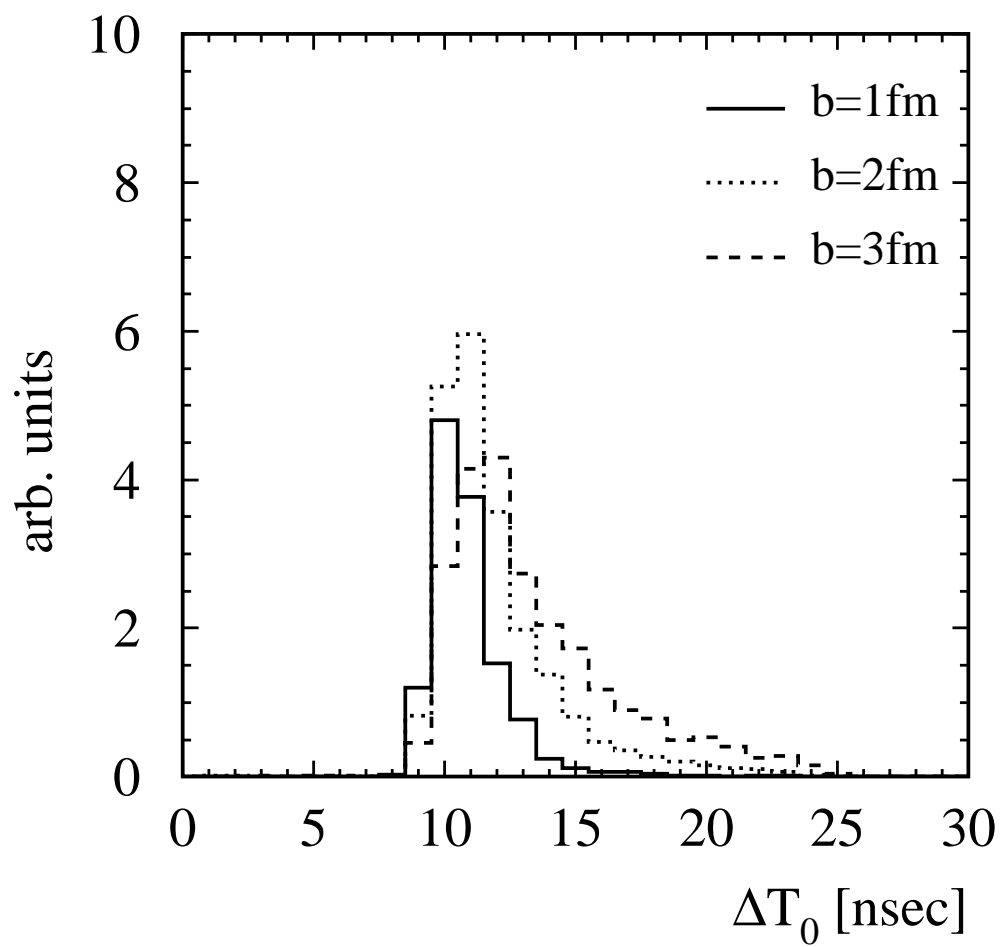


FIG.8

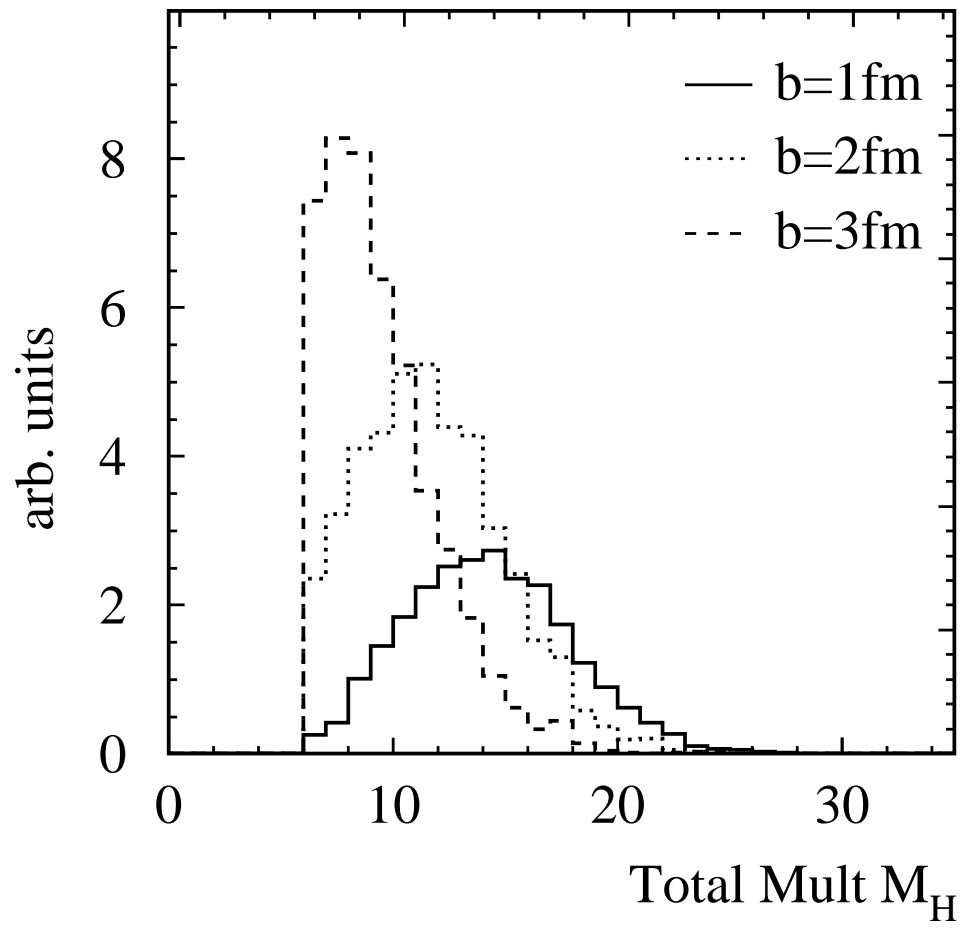


FIG.9

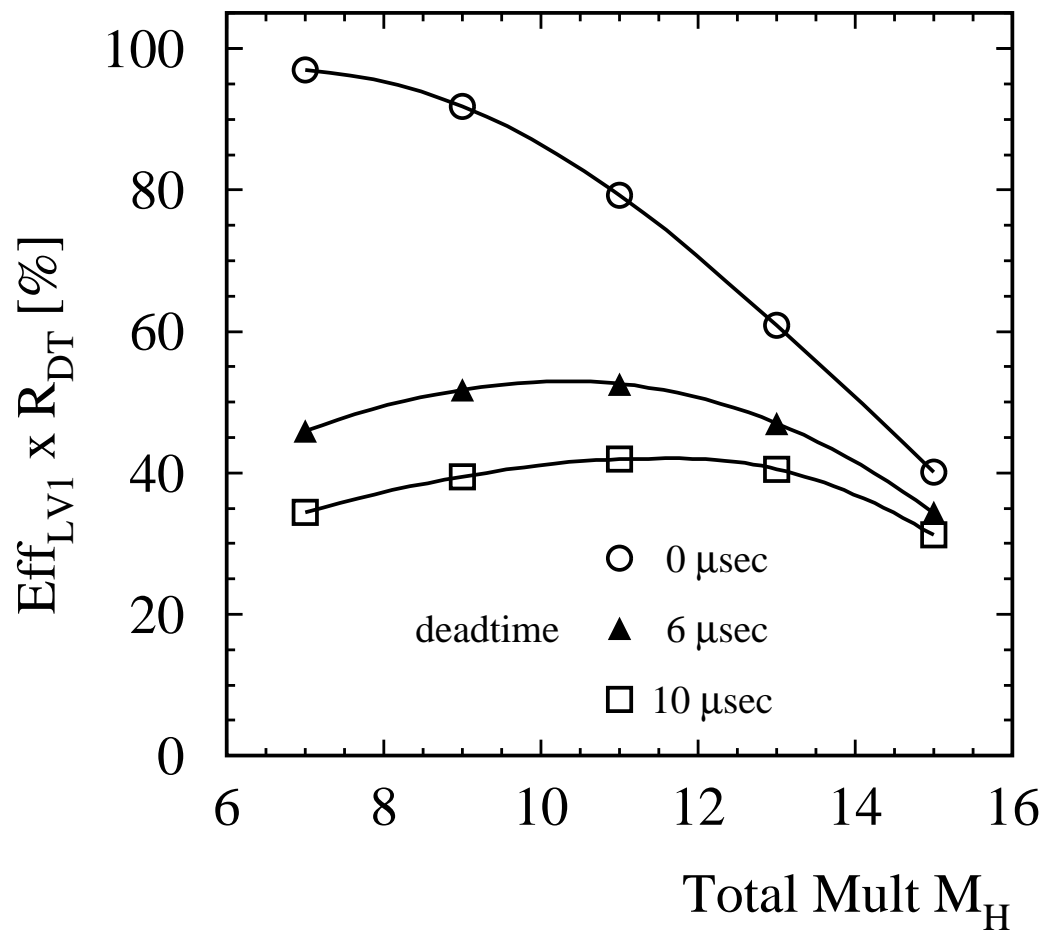


FIG.10

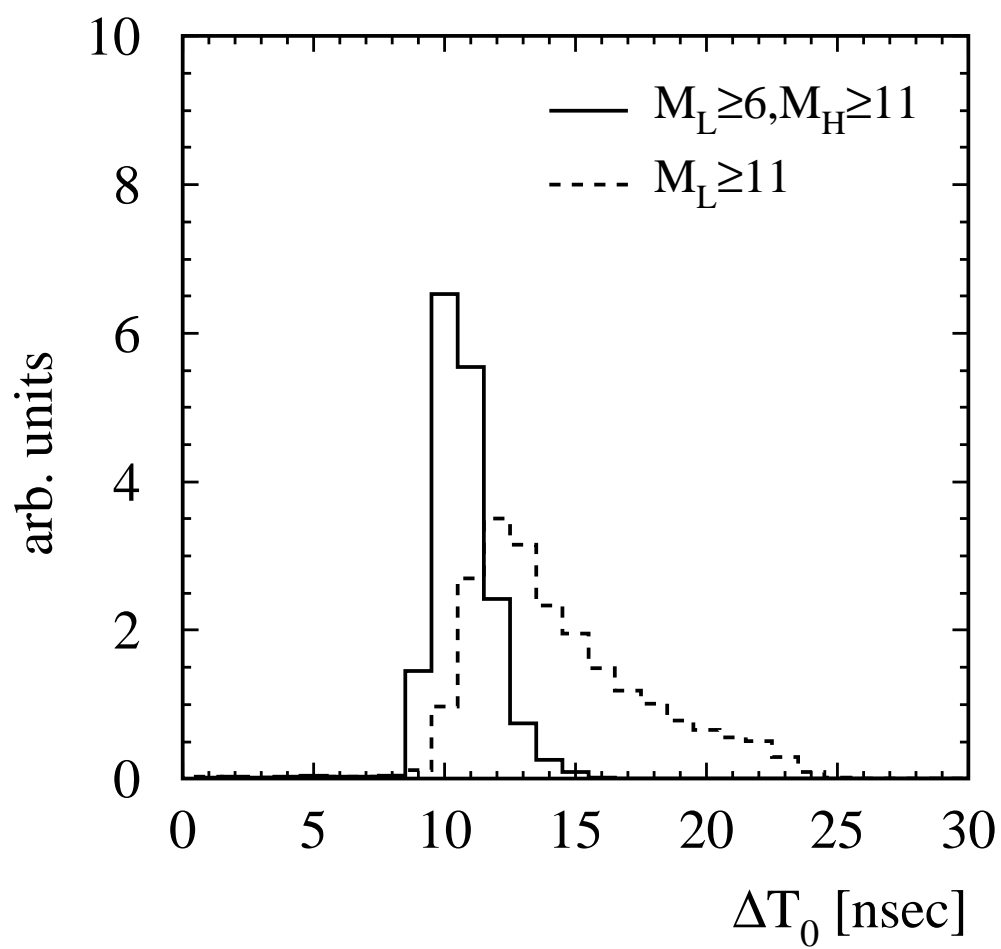


FIG.11